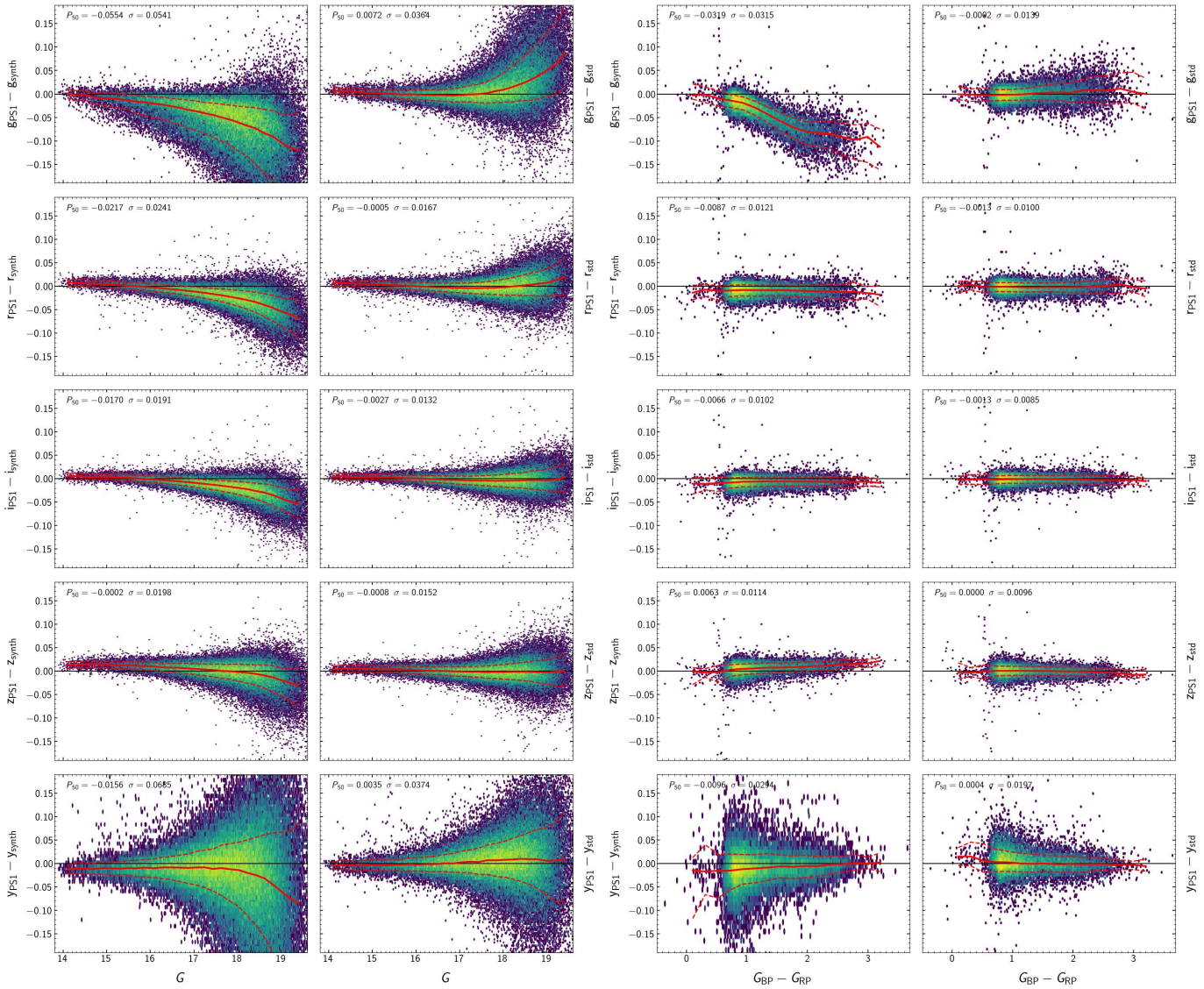

Fig. G.3. Performance and standardisation of PS1 *griz* bands XP synthetic magnitudes using the reference sample described in Sect. 3.4. The arrangement of the plots and symbols are the same as Fig. G.1.

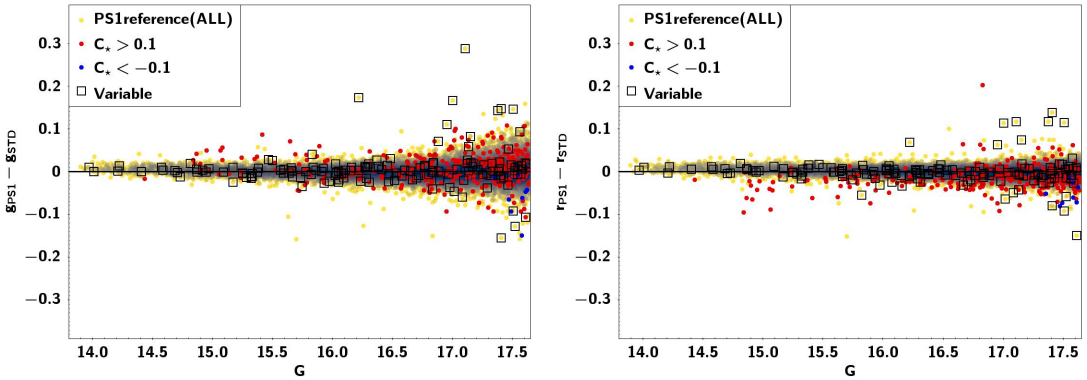

Fig. G.4. Example of the different distribution of $C_\star$ in Δmag in different passbands using the PS1 reference sample. We note that source with high positive $C_\star$ tend to have positive residuals in g_{PS1} and negative residuals in r_{PS1}. Also, most of the outliers in both plots are accounted for by sources with (relatively) large absolute $C_\star$ values and by sources classified as variable (see also Fig. 8).

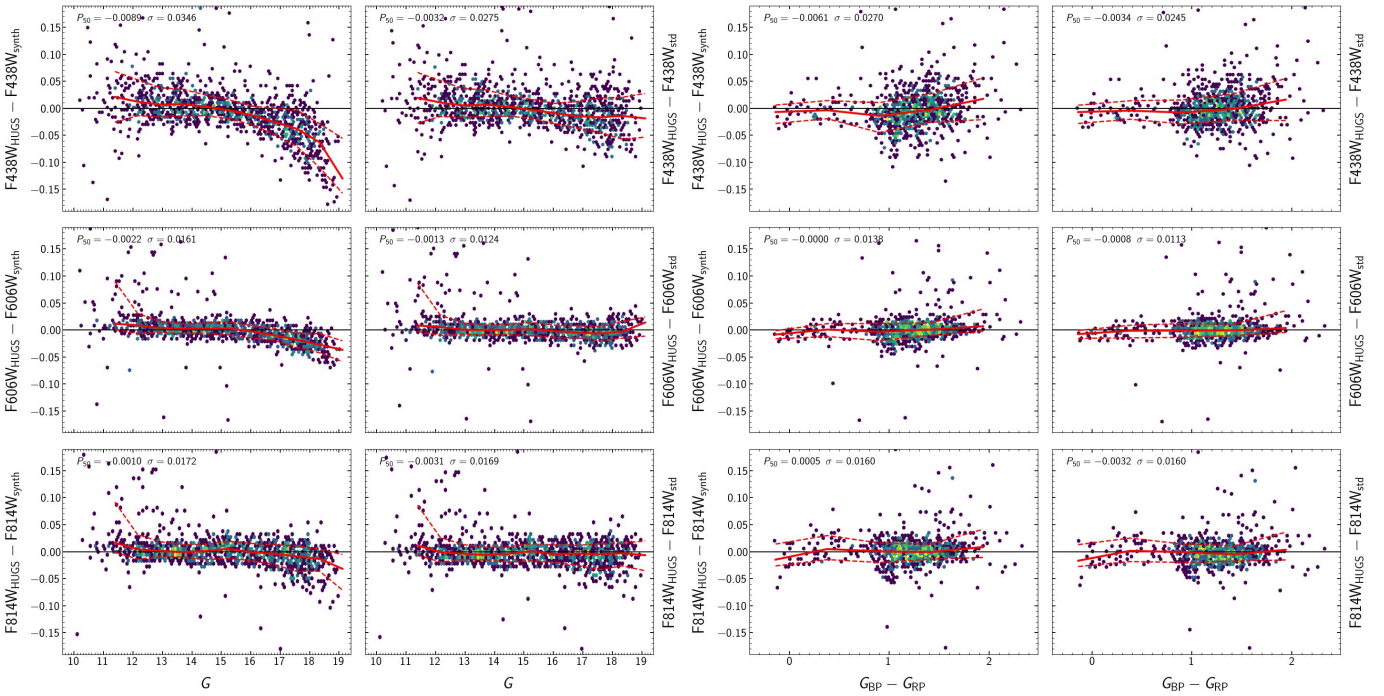

Fig. G.5. Performance and standardisation of HST F438W$_{WFC3/UVIS}$, F606W$_{ACS/WFC}$, and F814W $_{ACS/WFC}$ bands XP synthetic magnitudes using the reference sample described in Sect. 3.5. The arrangement of the plots and symbols are the same as Fig. G.1, above.

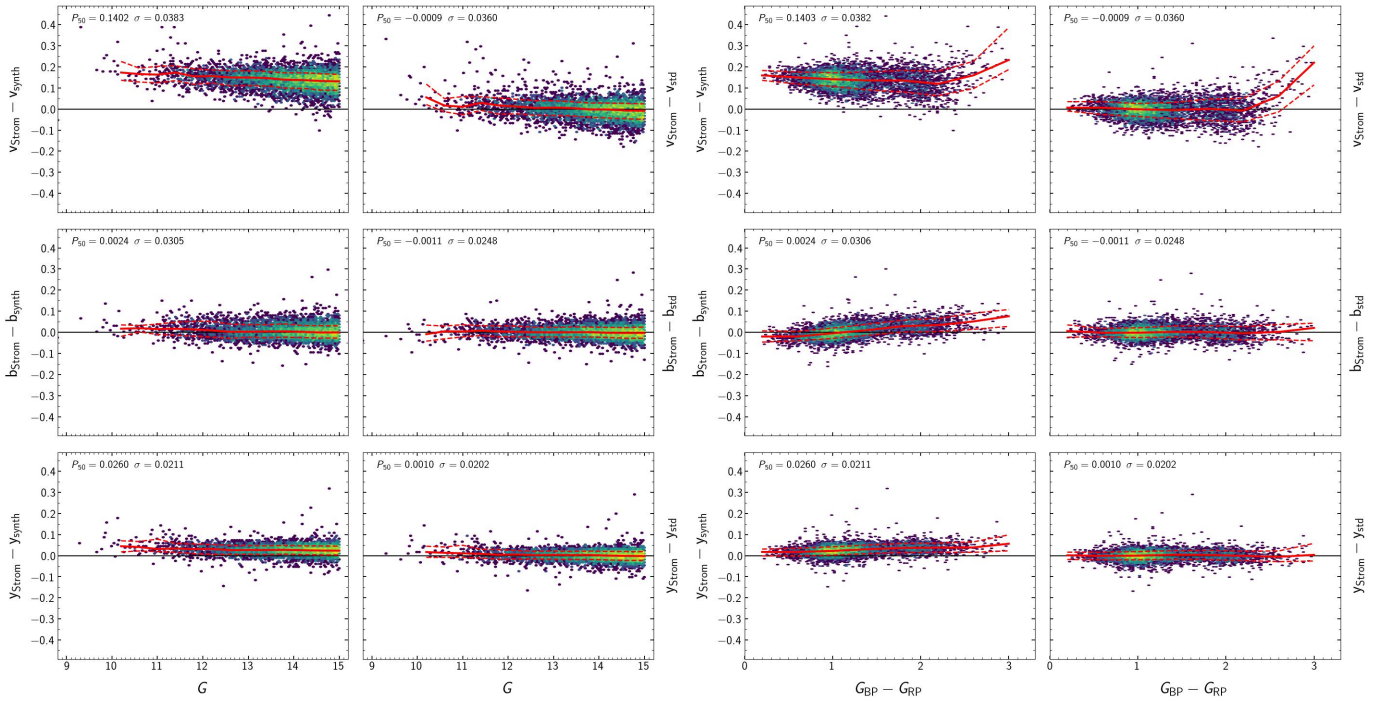

Fig. G.6. Performance and standardisation of Stromgren vby XP synthetic magnitudes using the reference sample described in Sect. 4.1. The arrangement of the plots and symbols are the same as Fig. G.1, above.

Table G.3. Standardised Strömgren magnitudes: median (P_{50}) and 15.87% (P_{16}) and 84.13% (P_{84}) percentiles of the Δmag distributions of Fig. 15. $n_\star$ is the number of sources in the considered bin.

G mag	$P_{50}(\Delta v)$ mmag	P_{16} mmag	P_{84} mmag	$P_{50}(\Delta b)$ mmag	P_{16} mmag	P_{84} mmag	$P_{50}(\Delta y)$ mmag	P_{16} mmag	P_{84} mmag	$n_\star$
11.2	31.7	-9.1	67.3	15.3	-10.5	44.1	16.6	-5.1	40.1	67
11.6	18.6	-21.6	52.9	1.9	-23.2	27.9	2.7	-18.1	28.6	125
12.0	12.5	-22.8	43.4	5.4	-19.7	26.6	5.2	-16.6	23.3	177
12.5	8.7	-26.5	44.4	0.9	-22.1	27.6	2.0	-16.9	21.6	289
12.9	7.3	-29.5	35.7	-0.4	-21.2	23.1	1.6	-17.1	19.9	448
13.3	7.0	-29.3	39.0	1.1	-23.5	28.3	3.3	-17.8	21.2	596
13.7	-0.2	-39.5	30.5	1.6	-21.5	25.7	2.1	-18.4	20.0	882
14.1	-2.9	-40.5	27.3	-2.4	-24.3	22.9	-0.3	-20.6	19.8	1111
14.6	-6.1	-44.7	27.0	-2.2	-26.9	22.9	-1.8	-22.3	18.7	1419
15.0	-7.4	-48.6	25.7	-2.2	-28.4	26.0	-1.9	-23.2	19.1	981

Appendix H: Reddening correction for C1 passbands

In this section, we provide the coefficients of the reddening curve to correct magnitudes in the C1 system (Sect. 4.4) for interstellar extinction. These are obtained by fitting polynomial functions to suitable theoretical simulations. To perform these simulations we used BTSettl library (Allard et al. 2013) retrieved from the Spanish Virtual Observatory web server for theoretical spectra[34].

Once the C1 photometry is simulated using BTSettl SEDs as input, we fit some polynomial dependencies to derive the absorption in any X band as a function of the global absorption in G-band, A_G, the $G_{BP} - G_{RP}$ colour, and considering also a crossed term between both (see Eq. H.1).

$$\frac{A_X}{A_G} = \alpha + \sum_{i=1}^{4} \beta_i \cdot (G_{BP} - G_{RP})^i + \sum_{j=1}^{3} \gamma_j \cdot A_G^j + \delta \cdot (G_{BP} - G_{RP}) \cdot A_G. \tag{H.1}$$

Figures H.1 and H.3 show the obtained fitted laws for every C1M medium and C1B broad passbands, respectively. The coefficients obtained for all C1 passbands are included in Table H.1. Although we produced the fitting using also extremely red sources (brown dwarfs) present in the BTSettl library, we recommend restricting the applicability of these relationships to the intervals plotted in the figures ($G_{BP} - G_{RP} < 5$ mag). The residuals obtained with these polynomials for every passband are plotted in Figs. H.2 and H.4 for C1M and C1B, respectively.

Table H.1. Coefficients obtained when fitting Eq. H.1 to the passbands in the C1 system using the BTSettl SED library (Allard et al. 2013).

X	α	β_1	β_2	β_3	β_4	γ_1	γ_2	γ_3	δ
$\frac{A_{C1M326}}{A_G}$	1.710	0.237	0.0131	-0.00325	0.000131	-0.0631	0.000303	-0.0000476	-0.000302
$\frac{A_{C1M379}}{A_G}$	1.533	0.257	0.00999	-0.00315	0.000134	-0.0736	-0.0000418	-0.0000625	0.00168
$\frac{A_{C1M395}}{A_G}$	1.492	0.249	0.00892	-0.00291	0.000124	-0.0716	0.000463	-0.0000892	0.00141
$\frac{A_{C1M410}}{A_G}$	1.442	0.241	0.00985	-0.00301	0.000127	-0.0686	-0.000266	-0.0000432	0.00158
$\frac{A_{C1M467}}{A_G}$	1.233	0.207	0.00768	-0.00251	0.000107	-0.0582	-0.000239	-0.0000369	0.00147
$\frac{A_{C1M506}}{A_G}$	1.117	0.0187	0.00745	-0.00229	0.0000981	-0.0550	0.000577	-0.0000748	0.000623
$\frac{A_{C1M515}}{A_G}$	1.089	0.183	0.00658	-0.00213	0.0000905	-0.0516	0.0000669	-0.0000440	0.000948
$\frac{A_{C1M549}}{A_G}$	1.009	0.169	0.00671	-0.00206	0.0000868	-0.0474	-0.000147	-0.0000277	0.000899
$\frac{A_{C1M656}}{A_G}$	0.825	0.139	0.00519	-0.00167	0.0000708	-0.0412	0.000448	-0.0000675	0.000898
$\frac{A_{C1M716}}{A_G}$	0.733	0.122	0.00438	-0.00143	0.0000614	-0.0363	0.000402	-0.0000608	0.000821
$\frac{A_{C1M747}}{A_G}$	0.683	0.114	0.00438	-0.00137	0.0000583	-0.0336	0.000407	-0.0000535	0.000515
$\frac{A_{C1M825}}{A_G}$	0.567	0.0953	0.00359	-0.00116	0.0000490	-0.0266	-0.000234	-0.00000838	0.000698
$\frac{A_{C1M861}}{A_G}$	0.523	0.0878	0.00310	-0.00105	0.0000449	-0.0264	0.000364	-0.0000513	0.000672
$\frac{A_{C1M965}}{A_G}$	0.433	0.0723	0.00259	-0.000885	0.0000380	-0.0218	0.000238	-0.0000400	0.000679
$\frac{A_{C1B431}}{A_G}$	1.367	0.183	0.0126	-0.00260	0.000101	-0.0486	0.00117	-0.0000154	-0.00372
$\frac{A_{C1B556}}{A_G}$	1.011	0.151	0.00628	-0.00167	0.0000678	-0.0423	0.00116	-0.0000564	-0.00157
$\frac{A_{C1B655}}{A_G}$	0.828	0.138	0.00458	-0.00166	0.0000711	-0.0393	-0.000192	-0.0000291	0.00138
$\frac{A_{C1B768}}{A_G}$	0.661	0.106	0.000155	-0.00101	0.0000480	-0.0306	-0.000148	-0.0000417	0.00226
$\frac{A_{C1B916}}{A_G}$	0.473	0.0789	0.00239	-0.000900	0.0000390	-0.0235	0.000268	-0.0000409	0.000657

[34] http://svo2.cab.inta-csic.es/theory/newov2/

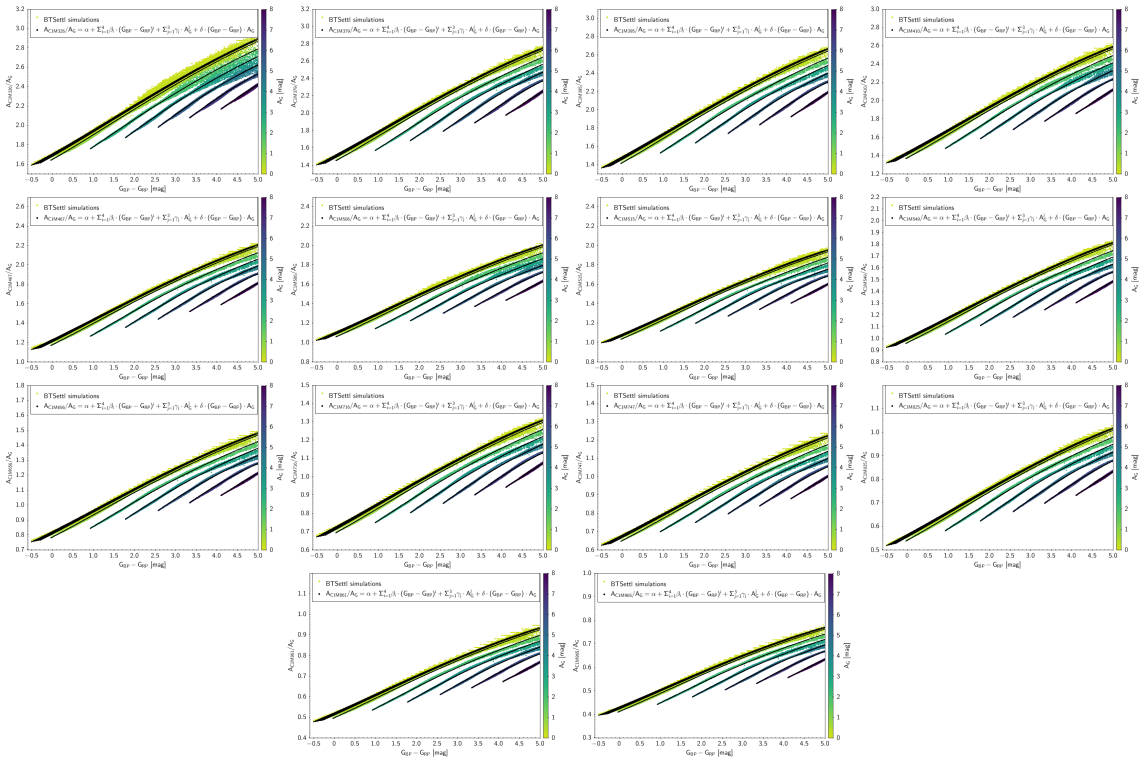

Fig. H.1. Fitted relationships (in black) obtained for the simulated C1M photometry using the BTSettl library (coloured points as a function of absorption in Gaia EDR3 *G* passband as derived by DPAC).

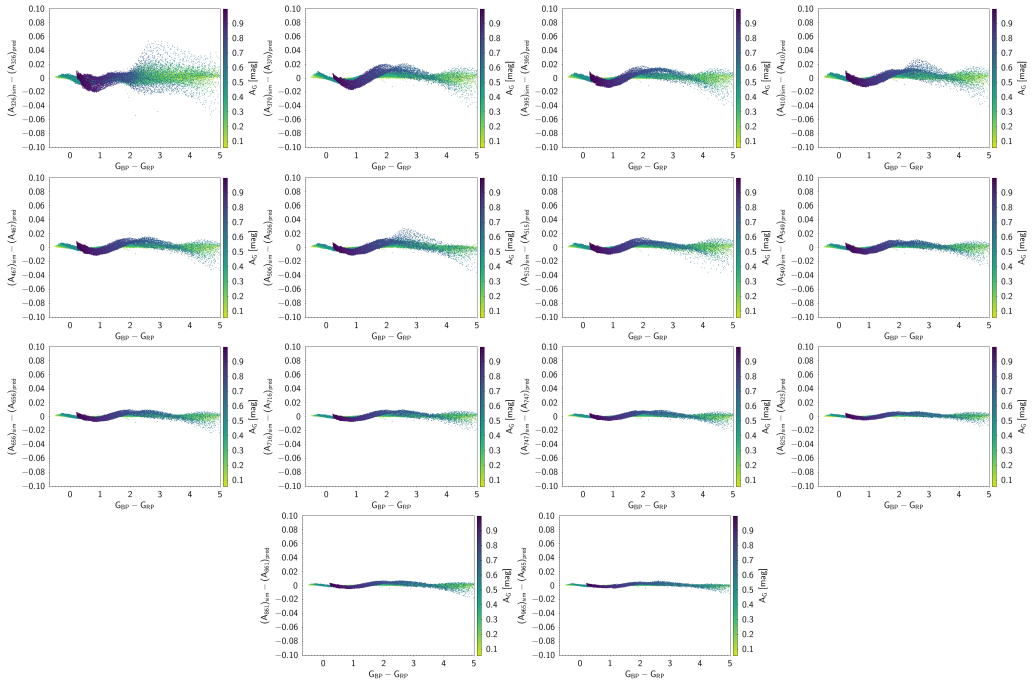

Fig. H.2. Residuals obtained for the fitted relationships in Fig. H.1.

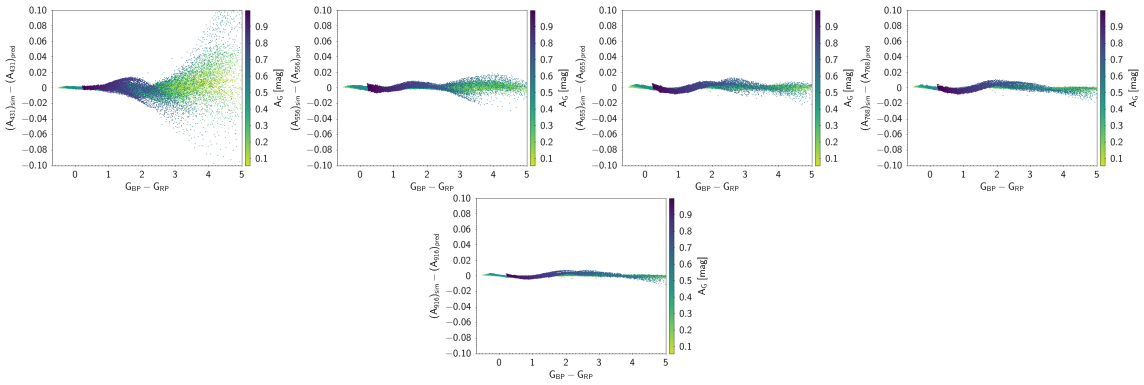

Fig. H.3. Same as Fig. H.1 but for C1B photometry.

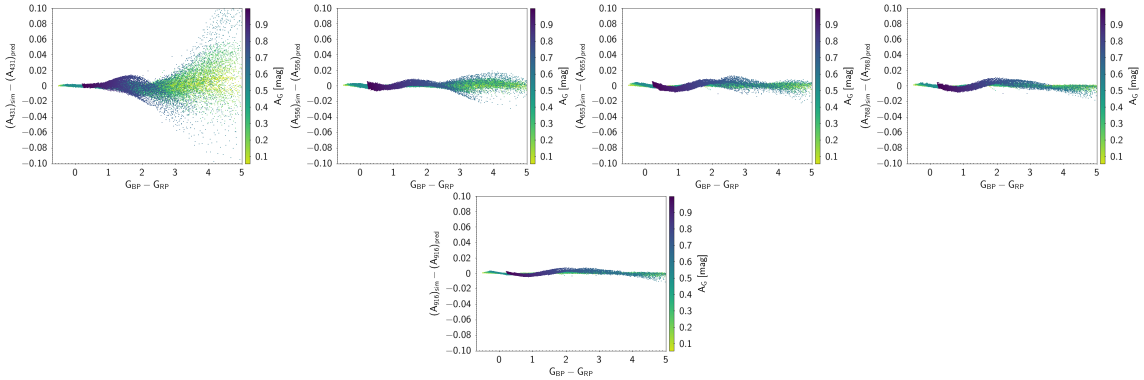

Fig. H.4. Same as Fig. H.4 but for C1B photometry.

Appendix I: *Gaia*-related acronyms

For convenience, we list all the *Gaia*-related acronyms used in this paper in Table I.1.

Table I.1. *Gaia*-related acronyms used in the paper. Each acronym is also defined at its first occurrence in the paper.

Acronym	Description	See
Apsis	Astrophysical parameter inference system	4.4
BP	Blue Photometer	Sect. 1
CU(s)	Calibration Unit	Sect. 1
DPAC	Data Processing and Analysis Consortium	Sect. 1
ECS	Externally Calibrated (XP) Spectra	Sect. 1
ELS	Emission Line Star	4.3
ESA	European Space Agency	Sect. 1
ESP-ELS	DR3 module dealing with ELS	4.3
FoV(s)	Field(s) of View	Sect. 3.5
G, G_{BP}, G_{BP}	Integrated *Gaia* magnitudes/fluxes	Sect. 2.2
GCNS	*Gaia* Nearby Stars Catalogue	Sect. 4.4
GSPC	*Gaia* Synthetic Photometry Catalogue	Sect. 6.2
GSPC-WD	*Gaia* Synthetic Photometry Catalogue for White Dwarfs	Sect. 6.3
GSP-Phot	DR3 module deriving astrophysical parameters from XP spectra	Sect. 5
GSP-Spec	DR3 module deriving astrophysical parameters from RVS spectra	Sect. 5
LSF	Line Spread Function	Sect. 1
PVL	Passband Validation Library	Sect. B
RP	Red Photometer	Sect. 1
RVS	Radial Velocity Spectrometer	Sect. 5.1
SPSS	*Gaia* Spectro Photometric Standard Stars	Sect. 1
XP	BP and RP (referred to spectra or photometry)	Sect. 1
XPSP	synthetic photometry from XP spectra	Sect. 1